RSPO/LGR signaling mediates astrocyte-induced proliferation of adult hippocampal neural stem cells

Daniela Valenzuela-Bezanilla, Muriel D. Mardones, Maximiliano Galassi, Sebastian B. Arredondo, Sebastian H. Santibanez, Nicolás Merino-Véliz, Fernando J. Bustos and Lorena Varela-Nallar*.

Institute of Biomedical Sciences (ICB), Faculty of Medicine and Faculty of Life Sciences, Universidad Andres Bello, Santiago, Chile.

Running title: RSPO/LGR signaling in adult neural stem cells

*Correspondence: Lorena Varela-Nallar, Echaurren 183, Postal code: 8370071, Santiago, Chile, Email: lorena.varela@unab.cl.

ABSTRACT

In the dentate gyrus of the adult hippocampus, neurogenesis from neural stem cells (NSCs) is regulated by Wnt signals from the local microenvironment. The Wnt/β-catenin pathway is active in NSCs, where it regulates proliferation and fate commitment, and subsequently its activity is strongly attenuated. The mechanisms controlling this pattern of activity are poorly understood. In stem cells from adult peripheral tissues, secreted R-spondin proteins (RSPO1-4) interact with LGR4-6 receptors and control Wnt signaling strength. Here, we found that RSPO1-3 and LGR4-6 are expressed in the adult dentate gyrus and in cultured NSCs isolated from the adult mouse hippocampus. The expression of LGR4-5 decreased in NSCs upon differentiation, concomitantly with the reported decrease in Wnt activity. Treatment with RSPO1-3 increased hippocampal NSCs proliferation and the expression of the Wnt target gene Cyclin D1. Moreover, RSPO1-3 were expressed by primary cultures of dentate gyrus astrocytes, a crucial component of the neurogenic niche able to induce NSC proliferation and neurogenesis. In co-culture experiments, astrocyte-induced proliferation of NSCs was prevented by RSPO2 knockdown in astrocytes, and by LGR5 knockdown in hippocampal NSCs. Altogether, our results indicate that RSPO/LGR signaling is present in the dentate niche, where it could control Wnt activity and proliferation of NSCs.

Keywords: Adult neurogenesis, hippocampus, neural stem cells, astrocyte, R-spondin, LGR receptors, Wnt.

INTRODUCTION

In the adult brain, neural stem cells (NSCs) are present in the subgranular zone (SGZ) of the hippocampal dentate gyrus. NSCs proliferate and differentiate into excitatory glutamatergic granule neurons that integrate into the dentate gyrus circuit and contribute to hippocampal function, a process termed adult hippocampal neurogenesis (Anacker and Hen 2017; Toda and Gage 2018; Kempermann 2022). The generation of functional adult-born granule neurons implies a fine-tuned regulation of the multiple steps of neurogenesis, including proliferation, fate commitment, differentiation, and maturation. NSCs in the SGZ are mostly quiescent (Shin et al. 2015; Urban and Cheung 2021), and once activated, they divide to generate actively proliferating neural progenitor cells (NPCs) that become neuroblasts, which differentiate into immature neurons and then into mature granule cells (Bonaguidi et al. 2011; Encinas et al. 2011).

The stages of neurogenesis are regulated by signaling factors secreted by different cell types found in the dentate niche. Among these factors, Wnt proteins play multiple roles during the process of neurogenesis [reviewed in (Arredondo et al. 2020b)]. Moreover, astrocytes that are major components of the adult dentate gyrus (Rieskamp et al. 2022), are known to regulate the maintenance of adult NSCs and induce neurogenesis in a Wnt-dependent manner (Lie et al. 2005; Wexler et al. 2009; Okamoto et al. 2011). Wnts are secreted glycoproteins that bind to seven-pass transmembrane Frizzled (FZD) receptors, which can trigger the canonical Wnt/β-catenin signaling pathway, or the non-canonical (β-catenin-independent) signaling cascades (Kohn and Moon 2005; Gordon and Nusse 2006; Butler and Wallingford 2017). Activation of the canonical Wnt/β-catenin signaling involves the formation of a ternary complex composed of Wnt, FZD, and the co-receptor low density lipoprotein receptor-related protein 5 or 6 (LRP5/6). Wnt stimulation results in the stabilization and

nuclear import of β-catenin, which acts as a transcriptional co-activator interacting with members of the T cell factor/lymphoid enhancer binding factor (TCF/LEF) family of transcription factors to induce the expression of Wnt target genes (e.g., CyclinD1 and Axin2 (Shtutman et al. 1999; Jho et al. 2002; Lustig et al. 2002)). The Wnt/β-catenin pathway controls cell fate decisions during embryonic development and in adult organisms, acting as a stem cell niche signal in many tissues (Gordon and Nusse 2006; Nusse and Clevers 2017). In adult neurogenesis, Wnt/β-catenin signaling controls proliferation and fate commitment of neural precursor cells (Kuwabara et al. 2009; Mao et al. 2009; Wexler et al. 2009; Qu et al. 2013; Austin et al. 2021), and in maturing newborn neurons, it regulates dendritic arbor complexity (Heppt et al. 2020). The role of the Wnt proteins has been studied in cultured NSCs isolated from the adult mouse hippocampus. These cells can differentiate into neurons or glial cells (Babu et al. 2011), and represent a controlled *in vitro* system to evaluate neurogenesis. In hippocampal NSCs, Wnt proteins induce cell proliferation through the expression of CyclinD1 (Wexler et al. 2009; Qu et al. 2013; Austin et al. 2021) and fate commitment through the expression of Neurogenin 2 (Ngn2) and NeuroD1 (Kuwabara et al. 2009; Qu et al. 2013; Amador-Arjona et al. 2015).

Wnt/β-catenin reporter mice have shown that this signaling pathway is active in NSCs, but then its activity is strongly attenuated (Lie et al. 2005; Garbe and Ring 2012; Heppt et al. 2020; Austin et al. 2021), which was proposed to be important for the proper dendritogenesis of newborn neurons (Heppt et al. 2020). The mechanisms involved in the dynamics of Wnt/β-catenin signaling during the early stages of adult neurogenesis are poorly understood. During development and in adult peripheral tissues, the strength of the Wnt/β-catenin signaling pathway is tightly regulated by the roof plate-specific spondin (R-spondin, RSPO) proteins (de Lau et al. 2012). RSPOs are a family of four cysteine-rich secreted glycoproteins

(RSPO1-4) that interact with the cell surface leucine-rich repeat-containing G protein-coupled receptors (LGR4-6) and with the transmembrane E3 ubiquitin ligases zinc and ring finger 3 (ZNRF3) or ring finger protein 43 (RNF43), which in the absence of RSPO ubiquitinate FZDs inducing their endocytosis and degradation (Carmon et al. 2011; de Lau et al. 2011; Glinka et al. 2011; Gong et al. 2012; Zebisch and Jones 2015). RSPO/LGR interaction prevents FZD ubiquitination, thereby augmenting Wnt/β-catenin signaling activity (Hao et al. 2012; Koo et al. 2012; Schuijers and Clevers 2012). Through this mechanism, RSPO proteins control proliferation and differentiation of stem cells in several adult tissues, including the intestine, stomach, hair follicles, and liver, among others (de Lau et al. 2014; Nagano 2019). Whether RSPO/LGR signaling plays a role in adult NSC behavior and adult neurogenesis is unknown. Here, we studied whether RSPO proteins and LGR receptors are expressed in the adult mouse dentate gyrus and evaluated whether RSPO proteins regulate proliferation of hippocampal NSCs. In addition, we evaluated the role of RSPO signaling in astrocyte-induced proliferation of neural precursors. Our results strongly suggest that RSPO/LGR is part of the signaling mechanisms present in the adult dentate niche that control the proliferation of NSCs.

RESULTS

RSPO proteins and LGR receptors are expressed in the adult mouse dentate gyrus

To investigate whether RSPO signaling exists in the dentate niche, we evaluated the expression of RSPO proteins and their LGR4-6 receptors in the dentate gyrus of 2-month-old mice. RSPO1-3 mRNA and protein levels were analyzed by RT-qPCR and immunoblotting (Fig. 1A-C). The variations in molecular weights, and the presence of more than one band are expected due to glycosylation of RSPO proteins. Structurally, these

proteins comprise an N-terminal signal peptide, two cysteine-rich furin-like domains (Fu1 and Fu2), followed by a thrombospondin type 1 repeat domain (TSR-1), an a basic charged C-terminal tail (Kim et al. 2006; Zebisch et al. 2013). RSPO1 and RSPO3 are both N-glycosylated at N137 in the Fu2 domain, and RSPO2 is N-glycosylated at N160 in the TSR-1 domain, which are crucial for efficient folding for secession (Chang et al. 2016). LGR4-6 mRNAs were also detected in the adult mouse dentate gyrus (Fig. 1A, B), and LGR4-5 were assessed at the protein level (Fig. 1C).

The distribution of RSPO proteins in the dentate gyrus was investigated by immunofluorescence staining. RSPO1 was mainly detected in the middle and outer thirds of the granule cell layer (GCL) and in the molecular layer (Fig. 1D), suggesting RSPO1 is distributed close to the dendritic arbor of granule cells. In agreement, co-distribution of RSPO1 with dendrites of immature neurons positive for doublecortin (DCX) was found in the GCL (Fig. 1D). Even though there was also RSPO2 staining in the middle and outer thirds of the GCL, it was mainly detected in the hilus (Fig. 1E). RSPO3 staining showed a low and homogenous distribution in the GCL, molecular layer, and hilus (Fig. 1E), and was detected in the SGZ (Fig. 1E).

RSPOs staining was also evaluated in the CA3 region, where the axons of newborn neurons are projected (Zhao et al. 2006). RSPO1 staining showed a somatodendritic distribution in CA3 neurons; RSPO2 staining was mainly observed in the *stratum lucidum*, suggesting an axonal distribution in mossy fibers; and RSPO3 showed a very low staining in CA3 neurons (Supplemental Fig. S1).

Altogether, our data indicate that RSPO proteins and LGR receptors are expressed in the adult mouse dentate gyrus, suggesting that RSPO/LGR signaling occurs in the dentate niche.

RSPO proteins induce proliferation of adult hippocampal NSCs

Considering that RSPO1-3 are expressed in the dentate gyrus, we evaluated whether these proteins regulate adult NSCs. For this experiment, we used cultured NSCs isolated from the adult mouse hippocampus as an *in vitro* model of neurogenesis (Babu et al. 2011; Arredondo et al. 2020a). We found that these cells express RSPO1-3 mRNA and protein (Fig. 2A-C). The expression of LGR4-6 mRNA was detected by RT-qPCR, and the results suggest that LGR6 exhibited the lowest level of expression in NSCs (Fig. 2A, B). LGR4-5 proteins were determined by immunoblotting (Fig. 2C) and immunostaining (Fig. 2D). LGR4-5 staining was detected in all cells positive for the neural stem/progenitor cell marker Nestin (Fig. 2C), indicating that hippocampal NSCs express the receptors for RSPO proteins. Interestingly, upon differentiation induced by growth factors withdrawal, LGR4-5 mRNA levels decreased significantly (Fig. 2E, F), while the mRNA of the neuronal marker Ngn2 increased (Fig. 2G). In addition, LGR5 protein levels significantly decreased, and LGR4 tended to decrease upon differentiation (Fig. 2H-K), which coincided with an increase in the immature neuronal marker DCX (Fig. 2H, I). These results indicate that the expression of LGR receptors is reduced upon differentiation, suggesting that RSPO/LGR signaling might have a role in proliferative NSCs.

To evaluate the effect of RSPOs on proliferation, NSCs were treated for 24 hours with 100 ng/ml recombinant RSPO1 (rRSPO1), rRSPO2, or rRSPO3 and incubated with the nucleotide analog BrdU for the last 2 hours of treatment. The incorporation of BrdU was analyzed by immunofluorescence staining (Fig. 3A). The percentage of BrdU positive cells was significantly increased in NSCs treated with rRSPO1-3 (Fig. 3B-D), indicating that treatment with RSPOs induced proliferation.

RSPOs potentiate Wnt signaling activity by augmenting the sensitivity of cells to Wnt ligands (Schuijers and Clevers 2012). Therefore, the effect of rRSPOs likely involves the enhancement of endogenous Wnt ligands action (Wexler et al. 2009). Intriguingly, we found that co-treatment with rRSPO1-3 plus recombinant Wnt3a (rWnt3a) ligand, known to induce proliferation of hippocampal NSCs (Wexler et al. 2009), did not augment the effect of rWnt3a (Fig. 3E-G and Supplemental Fig. S2). This result indicates that RSPOs were not able to augment the effect of an exogenous Wnt on NSCs proliferation.

To evaluate whether treatment with rRSPOs alone or in combination with rWnt3a induced Wnt/β-catenin signaling activity, the expression of Wnt target genes was assessed by RT-qPCR. For this experiment, NSCs were treated with 100 ng/ml rRSPOs in the presence or absence of 150 ng/ml rWnt3a for 24 hours (Fig. 3H-K). We evaluated the expression of CyclinD1, previously shown to mediate the proliferative effect of Wnt/β-catenin signaling on cultured hippocampal NSCs (Qu et al. 2013). We found that treatment with rRSPO1-3 significantly increased CyclinD1 mRNA levels (Fig. 3H) but did not increase the effect of rWnt3a, in agreement with the finding that co-treatment did not potentiate the effect on proliferation (Fig. 3E-G). Interestingly, the expression of Axin2, a well-described Wnt target gene (Jho et al. 2002; Leung et al. 2002), was not induced by treatment with rRSPO1-3, while treatment with rWnt3a alone or in the presence of rRSPOs significantly increased Axin2 mRNA levels (Fig. 3I). Axin2 is a component of the complex that induces the degradation of β-catenin and, therefore, is a target gene that functions in a negative feedback loop to limit Wnt signaling activation (Jho et al. 2002; Lustig et al. 2002). Furthermore, treatment with rWnt3a alone or with rRSPOs strongly induced the expression of RNF43 (Fig. 3J), which also induces a negative feedback loop for Wnt activity through ubiquitination of FZD

receptors (Koo et al. 2012). These results suggest that treatment with rWnt3a ± rRSPOs induces a negative regulation of the Wnt/β-catenin signaling, which is not induced by treatment with rRSPOs alone.

We also found that co-treatment with rWnt3a ± rRSPO increased Ngn2 mRNA (Fig. 3K). Ngn2 is a target gene involved in Wnt-mediated neuronal differentiation of hippocampal NSCs (Qu et al. 2013; Amador-Arjona et al. 2015). Interestingly, previous reports have shown that high stimulation of Wnt/β-catenin signaling in proliferating NSCs reduces their proliferative capacity and promotes neuronal differentiation (Austin et al. 2021). In this context, the lack of potentiation on proliferation and CyclinD1 expression by co-treatment with rRSPOs plus rWnt3a could be attributed to an increase in differentiation induced by higher Wnt activity.

RSPO proteins mediate astrocyte-induced proliferation of adult hippocampal neural progenitor cells

Astrocytes are a crucial component of the dentate niche. *In vitro*, hippocampal astrocytes induce proliferation and neurogenesis of cultured NSCs (Song et al. 2002; Lie et al. 2005; Okamoto et al. 2011). To assess the potential role of RSPOs in the astrocyte-mediated induction of proliferation, we created sandwich co-cultures of NSCs with hippocampal astrocytes (NSC/Astro co-cultures), using a custom-made 3D-printed support (Supplemental Fig. S3A), in which cells shared the medium without direct contact with each other (Kaech and Banker 2006). For these experiments, astrocytes were isolated from the dentate gyrus of adult mice. As expected, these cells expressed the astrocytic markers GFAP and S100β

(Supplemental Fig. S3B), and induced proliferation of NSCs in co-culture experiments (Supplemental Fig. S3C).

We found that astrocytes extracted from the dentate gyrus expressed RSPO1-3 mRNAs (Fig. 4A, B) and proteins (Fig. 4C). To investigate the contribution of RSPO proteins in astrocyte-induced proliferation of hippocampal NSCs, NSCs/Astro co-cultures were performed for 24 hours in the presence or absence of soluble Fc-LGR4 or Fc-LGR5 chimeras consisting of the extracellular domain of LGR receptors fused to the Fc region of immunoglobulin (Fig. 4D). Soluble Fc-LGRs bind to RSPO proteins, preventing their action. Proliferation of NSCs co-cultured with astrocytes was significantly reduced in the presence of Fc-LGR4 or Fc-LGR5 but was not affected by the control Fc protein (Fc-Ctrl) (Fig. 4E and Supplemental Fig. S4A). This result suggests that RSPO proteins are involved in the astrocyte-induced proliferation of NSCs. Noteworthy, when NSCs were cultured alone (not in co-cultures) and incubated with Fc-LGRs, there was no effect on proliferation (Supplemental Fig. S4B), indicating that the decrease in proliferation induced by the treatment with Fc-LGR4-5 in NSC/Astro co-cultures was mediated by RSPO ligands secreted by astrocytes and not by NSC-derived RSPOs.

To further demonstrate the role of astrocyte-derived RSPOs on NSCs proliferation, we knocked down the expression of RSPO2, which is the most highly expressed in astrocytes (Fig. 4A, B). Knockdown was first assessed in Neuro2a (N2a) cells transduced with lentiviruses expressing two different shRNAs targeting RSPO2 (shR1 and shR2), or a control shRNA (shC), plus GFP. Both shR1 and shR2 significantly reduced RSPO2 protein levels compared with shC (Fig. 5A, B), and shR2 was selected for further experiments. In N2a cells, shR2 significantly reduced RSPO2 mRNA compared to control cells transduced with shC (Fig. 5C). Then, RSPO2 knockdown was assessed in astrocytes transfected with shC or shR2,

and RSPO2 protein levels were analyzed in total cell lysates and in the secreted media (Fig. 5D), since RSPO2 is a secreted glycoprotein. Remarkably, the immunoreactive bands observed in the media displayed a reduced molecular mass than the bands observed in the lysates (Fig. 5D). In both, cell lysates (Fig. 5E) and media (Fig. 5F), reduced RSPO2 levels were observed in astrocytes transfected with shR2, compared to shC (Fig. 5E, F).

To evaluate the role of RSPO2 in astrocyte-induced proliferation, NSCs were co-cultured for 24 hours with astrocytes transfected with shC or shR2, and proliferation was assessed by the expression of the mitotic marker Ki67 (Fig. 5G). Compared to NSCs cultured without astrocytes, co-culture with shC-expressing astrocytes significantly increased the percentage of NSCs positive for Ki67, an effect that was significantly decreased in NSCs co-cultured with shR2-expressing astrocytes (Fig. 5H). This result indicates that RSPO2 is required for proliferation induced by astrocytes.

To further assess the role of RSPO/LGR signaling in astrocyte-induced proliferation, LGR5 was knocked down in NSCs by transduction with a retrovirus expressing an shRNA targeting LGR5 (shLGR5). The retroviruses expressing shLGR5 or a control shRNA (shC) also expressed the fluorescent protein ZsGreen (ZsG). LGR5 mRNA and protein levels were significantly reduced in cells expressing shLGR5, compared to cells expressing shC (Fig. 6A-C). NSCs were then transduced with retrovirus expressing shC or shLGR5, and after 24 hours were co-cultured with astrocytes. Proliferation in transduced NSCs (ZsG+) was assessed by Ki67 staining (Fig. 6D). The percentage of ZsG+ cells positive for Ki67 was significantly reduced in LGR5-deficient NSCs compared to control cells expressing shC (Fig. 6E).

Altogether, these findings demonstrate that RSPO2 secreted by astrocytes and the LGR5 receptor expressed in hippocampal NSCs are crucial for astrocyte-induced proliferation of NSCs.

DISCUSSION

Our evidence suggests that RSPO signaling is part of the mechanisms that control the proliferation of neural precursor cells in the adult dentate niche. During development and in adult tissues, RSPO proteins enhance Wnt/β-catenin signaling. Secreted RSPOs interact with a LGR receptor and the E3 ubiquitin ligase ZNRF3 or RNF43 and induce the internalization and degradation of FZD receptors (Hao et al. 2012; Koo et al. 2012). This interaction triggers the membrane clearance of E3 ligase, which in the absence of RSPOs, ubiquitinates FZD receptors inducing their internalization and degradation [reviewed in (de Lau et al. 2014; Zebisch and Jones 2015; Nagano 2019)]. By augmenting Wnt activity, RSPOs exert critical functions in adult tissue homeostasis by controlling proliferation and fate commitment of stem cells in several peripheral tissues (Yan et al. 2017; Harnack et al. 2019; Sigal et al. 2019). Moreover, RSPOs have been used to induce tissue regeneration (Zhao et al. 2009; Zhang et al. 2020) and therefore, they have emerged as interesting therapeutic targets to be used in regenerative medicine applications. Our results suggest that RSPO signaling could be an interesting target to promote neurogenesis in physiological and pathological conditions including aging (Ben Abdallah et al. 2010; Knoth et al. 2010; Moreno-Jimenez et al. 2019), and neurodegenerative diseases (Moreno-Jimenez et al. 2019; Tobin et al. 2019; Terreros-Roncal et al. 2021; Zhou et al. 2022; Cao et al. 2023).

We determined that RSPO1-3 and their LGR4-6 receptors are expressed in the adult mouse dentate gyrus. In agreement with *in situ* hybridization data (Lein et al. 2007), RSPO4 was not detected by RT-qPCR, so this protein was not evaluated in the following experiments. Moreover, RSPO4 is the least active RSPO protein, as determined in cell-based Wnt signaling assays (Kim et al. 2008). Interestingly, the differential distribution of RSPO1-3 determined by immunostaining in hippocampal sections suggests that these ligands might play different roles in the hippocampus. Particularly, RSPOs expressed in the CA3 region might control the reactivation of Wnt signaling reported in mature neurons, as previously suggested (Heppt et al. 2020). Distinct patterns of expression (Nam et al. 2007), as well as divergent roles (Nagano 2019; Ter Steege and Bakker 2021), have been described for RSPOs at different developmental stages.

Furthermore, we found that LGR4-6 receptors are expressed in the dentate gyrus. LGRs have been identified as markers of stem cells in adult tissues (Barker et al. 2007; Jaks et al. 2008; Barker et al. 2010; Mustata et al. 2011; de Visser et al. 2012; Wang et al. 2013; Lehoczky and Tabin 2015; Blaas et al. 2016); however, LGR5 is also expressed in postmitotic cerebellar granule neurons during postnatal development (Miller et al. 2014) and postmitotic neurons in the adult olfactory bulb (Yu et al. 2017), and LGR4 is expressed in Purkinje cells of the cerebellum (Van Schoore et al. 2005) We found that LGR4-5 are expressed in proliferative hippocampal NSCs, suggesting that these cells are sensitive to RSPO proteins. Accordingly, treatment with recombinant RSPO1-3 significantly induced the proliferation of NSCs. RSPOs have previously been shown to be required for proliferation of intestinal stem cells (Kim et al. 2005; Chaves-Perez et al. 2022); RSPO overexpression induces proliferation of these cells, while RSPO inhibition induces lineage commitment and differentiation (Yan et al. 2017). Also, RSPOs increase proliferation of stomach cells (Sigal et al. 2017), adult

hair follicle dermal stem cells (Hagner et al. 2020), and lung epithelial stem/progenitor cells (Raslan et al. 2022).

Interestingly, we found that the expression of LGR4-5 receptors decreased upon NSC differentiation, suggesting that RSPO/LGR signaling is reduced after fate commitment. As previously reported, the activity of Wnt/β-catenin signaling also drops upon differentiation. In the dentate gyrus, Wnt/β-catenin activity declined in committed neural progenitors (Garbe and Ring 2012; Heppt et al. 2020; Austin et al. 2021), and in cultured hippocampal NSCs, the Wnt3a-induced TCF/LEF response was gradually downregulated throughout the first 2–3 days of differentiation (Schafer et al. 2015). Our results suggest that the downregulation of LGR4-5 expression upon NSC differentiation may contribute to the attenuation of the canonical Wnt/β-catenin signaling pathway observed in neural committed progenitors.

Considering that the action of RSPOs involves augmenting the sensitivity of cells to Wnt ligands (Kim et al. 2008), rRSPOs likely increased proliferation by amplifying basal activity of endogenous Wnt ligands expressed in adult hippocampal NSCs (Wexler et al. 2009). In response to rRSPOs treatment, we found increased mRNA levels of the Wnt target gene CyclinD1. Interestingly, we did not observe a potentiation of this effect on CyclinD1 expression or NSCs proliferation by co-treatment with rRSPOs plus rWnt3a. However, treatment with rWnt3a or co-treatment with rRSPOs plus rWnt3a did induce the expression of Axin2 and RNF43, which was not observed by treatment with rRSPOs alone. Both Axin2 and RNF43, are negative regulators of the Wnt/β-catenin signaling, acting at different levels of the Wnt pathway. Axin2 induces the degradation of β-catenin by functional interaction with APC and GSK-3β (Clevers and Nusse 2012) while RNF43 promotes the membrane clearance of FZD receptors (Koo et al. 2012). Mutations in these proteins result in aberrant

activation of the Wnt signaling pathway and are found in a variety of human cancers (Liu et al. 2000; Lustig et al. 2002; Hao et al. 2016). Our findings suggest that there is a tight control of Wnt/β-catenin activity in proliferative NSCs. On the one hand, positive signals allow the proliferation of NSCs, while negative feedback mechanisms that limit Wnt activity prevent excessive proliferation. In this context, our results suggest that low levels of Wnt activity induced by treatment with rRSPOs alone induce proliferation, while higher levels of Wnt activity induced by treatment with rWnt3a plus rRSPOs activate the negative feedback, thus blocking further proliferation. This agrees with previous findings in which stimulation of Wnt/β-catenin signaling with the GSK3β inhibitor CHIR99021 reduced the proliferative capacity of cultured hippocampal precursor cells while inducing a strong increase in Axin2 expression (Austin et al. 2021).

In addition, it was reported that high stimulation of Wnt/β-catenin signaling promotes the differentiation of hippocampal NSCs while reducing proliferation (Austin et al. 2021). Moreover, elevated and sustained β-catenin activation sequentially promotes the proliferation and subsequent differentiation of adult NSCs (Rosenbloom et al. 2020). We observed that treatment with Wnt3a ± rRSPOs increased the expression of Ngn2, suggesting that this treatment induced the differentiation of NSCs. In this context, our results suggest that lower levels of Wnt activity induced by treatment with rRSPOs alone induced proliferation, while higher levels of Wnt activity induced by treatment with Wnt3a ± rRSPOs promoted differentiation.

In addition to augmenting Wnt/β-catenin signaling, other ways of action have been described for RSPOs including modulation of non-canonical Wnt signaling (Glinka et al. 2011; Ohkawara et al. 2011; Scholz et al. 2016), and the antagonistic effect on BMP signaling (Lee

et al. 2020). We cannot exclude these mechanisms are also involved in the effect of rRSPOs on adult hippocampal NSCs.

Astrocytes are important components of the neurogenic niche that provides signaling molecules at the SGZ and also in the ML close to NSC projections (Sultan et al. 2015; Moss et al. 2016; Casse et al. 2018; Schneider et al. 2019; Arredondo et al. 2022). We determined that astrocytes isolated from the dentate gyrus of adult mice express RSPO1-3. We found that no-contact co-cultures of hippocampal NSCs with dentate gyrus astrocytes induced the proliferation of NSCs, which was prevented by: (i) co-incubation with the extracellular domains (Fc-chimera) of LGR4 or LGR5; (ii) knocking down the expression of RSPO2 in astrocytes; and (iii) knocking down the expression of LGR5 in NSCs. We knocked down the expression of RSPO2 since RT-qPCR data suggested this is the highest expressed RSPO in astrocytes (with lower delta CT value). Similarly, LGR5 was selected since RT-qPCR analysis suggested this is the most highly expressed LGR in NSCs; in addition, Fc-LGR5 strongly blocked proliferation induced by astrocytes.

These data strongly support that RSPO2/LGR5 signaling is involved in the previously described astrocytes-induced proliferation of hippocampal NSCs (Song et al. 2002; Lie et al. 2005; Okamoto et al. 2011). Interestingly, RSPO2 knockdown in astrocytes completely prevented the effect of co-culture on proliferation, even though there was an incomplete decrease of RSPO2 levels in the lysate and media. This suggests that there might be a concentration threshold for RSPO2 to induce proliferation. Additionally, treatment with Fc-LGR4-5 did not affect basal NSCs proliferation, when not in co-culture, possibly because the concentration of RSPOs secreted by NSCs is too low to mediate an autocrine effect. Similarly to what we propose for RSPO levels, Wnt concentration thresholds have been reported to be required for Wnt/β-catenin effects, including cell proliferation in the intestinal crypts (Dunn

et al. 2016), and lineage commitment in embryonic stem cells (Tsakiridis et al. 2014).

In summary, our results indicate that RSPO proteins are expressed in the adult dentate gyrus, and RSPOs secreted by dentate astrocytes promote proliferation of hippocampal precursor cells in an LGR-dependent manner. These data indicate that RSPO/LGR signaling might be part of the signaling mechanisms of the adult dentate niche.

MATERIALS AND METHODS

Animals

All procedures involving animals were performed according to the NIH and ARRIVE guidelines and were conducted with the approval of the Bioethics Committee of Universidad Andrés Bello (006/2019). Adult two-month-old female and male C57/BL6 mice were used for the experiments. Mice had access to water and food ad libitum in a 12:12 hours light/dark cycle.

RT-qPCR

Total RNA from NSCs, astrocytes, dentate gyrus, or N2a cells was extracted using TRIzol reagent (Life Technologies) and reversely transcribed into complementary DNA (cDNA) using M-MuLV reverse transcriptase (NEB.M0253S, New Englands BioLabs, Ipswich, MA). qPCR was performed using the Brilliant II SYBR Green QPCR master mix (Agilent Technologies, Santa Clara, CA). The primers used are listed in Supplemental Table S1. Gene expression was normalized to the endogenous housekeeping genes β-actin (ΔCt) and to control samples (ΔΔCt). Fold-change in mRNA levels was calculated using $2^{-\Delta\Delta CT}$ (Rao et al. 2013). For all samples, technical triplicates were carried out for each qPCR run and then averaged, and at least 3 independent experiments were performed.

Western blot analysis

Total protein extracts from the dentate gyrus, NSCs, or astrocytes were prepared as previously described (Arredondo et al. 2020a). Proteins were resolved in 10% SDS/PAGE, transferred to a PVDF membrane, blocked, and incubated overnight at 4ºC with primary antibodies: rabbit anti-DCX (4604, CellSignaling Technology Inc., 1:750), mouse anti-β-actin (A5441, Sigma-Aldrich, 1:10,000), rabbit anti-GFAP (Z0334, Dako, 1:1000), goat anti-RSPO1 (AF3474, R&D Systems, 1:200), rabbit anti-RSPO2 (MB59206616, MyBioSource, 1:500), rabbit anti-RSPO3 (PA5-38052, Invitrogen, 1:250), rabbit anti-LGR4 (PA5-67868, Invitrogen, 1:500), mouse anti-LGR5 (MA5-25644, Invitrogen, 1:2000), and rabbit anti-LGR5 (HPA012530, Atlas Antibodies, 1:500). Peroxidase-conjugated secondary antibodies (Invitrogen) were then used, and detected using the ECL technique (PerkinElmer, Waltham, MA).

Perfusion, postfixation, and tissue sectioning

Animals were anesthetized using a mixture of 200 mg/kg ketamine and 20 mg/kg xylazine and transcardially perfused with saline serum, followed by 4% paraformaldehyde (PFA, Sigma-Aldrich) in 0.1 M PBS. Brains were removed and postfixed in 4% PFA in PBS for 24 hours at room temperature, and then dehydrated in 30% sucrose. Brains were sectioned on a cryostat (Cryostat MEV, Slee).

Immunofluorescence staining

Immunostaining was carried out as previously described for tissue sections (Varela-Nallar et al. 2014) or cultured cells (Varela-Nallar et al. 2009; Abbott et al. 2013). The primary antibodies used were: mouse anti-GFAP (MA515086, Thermo Fischer Scientific, 1:8000), mouse anti-S100β (ab4066, Abcam, 1:100), rat anti-BrdU (ab6326, Abcam, 1:300), rat anti-

Ki67 (14-5698-82, Invitrogen, 1:250), mouse anti-Nestin (MAB353, Millipore, 1:50), goat anti-Sox2 (2748, Cell Signaling Technology Inc., 1:100), goat anti-DCX (SC-8066, Santa Cruz Biotechnology, 1:250), rabbit anti-DCX (4604, Cell Signaling Technology Inc., 1:750), goat anti-RSPO1 (AF3474, R&D Systems, 1:200), rabbit anti-RSPO2 (HPA024764, Sigma, 1:500), rabbit anti-RSPO3 (PA5-38052, Invitrogen, 1:150), rabbit anti-LGR4 (PA5-67868, Invitrogen, 1:250), and rat anti-LGR5 (MAB8240SP, R&D Systems, 1:50). As secondary antibodies, Alexa- and DyLight-conjugated antibodies were used. NucBlue (R37605, Invitrogen) was used as a nuclear dye. Image acquisition was performed using a Nikon Ti-E Microscope (Nikon, USA) or a Leica TCS SP8 (Leica Microsystems) confocal microscope using a 40x or 60x objective.

Isolation and culture of progenitors from the adult mouse hippocampus

NSCs were isolated from the hippocampus of 10 female 6-8-week-old C57/BL6 mice and cultured in monolayers, as previously described (Babu et al. 2011), with some modifications as in (Guerra et al. 2022). NSCs were plated at 10,000 cells/cm^2 in culture plates pretreated with poly-D-lysine (Merck) and laminin (Gibco), as previously described in (Guerra et al. 2022). NSCs were cultured in DMEM/F12 (Gibco), supplemented with B27 (Gibco), 100 U/ml penicillin and 100 µg/ml streptomycin (Gibco), and the growth factors FGF-2 (20 ng/ml, Alomone Labs) and EGF (20 ng/mL, R&D systems). NSC differentiation was induced withdrawal of these growth factors.

For proliferation analysis, NSCs were treated in the presence or absence of the recombinant proteins RSPO1 (7150-RS/CF, R&D Systems), RSPO2 (6946-RS/CF, R&D Systems), or RSPO3 (4120-RS/CF, R&D Systems) for 24 hours, and 5 µM BrdU (Sigma-Aldrich) was added for the last 2 or 4 hours of treatment. Proliferation was quantified as the percentage of BrdU-positive cells out of the total number of cells positive for the nuclear staining. For

differentiation analysis, NSCs were treated with recombinant proteins for 4 days in the absence of growth factors. Neuronal differentiation was quantified as the percentage of cells that expressed DCX.

Isolation and culture of astrocytes from the adult mouse dentate gyrus

Thew extraction of the dentate gyrus of 6-8-week-old mice was performed as previously described (Walker and Kempermann 2014), and then astrocytes were isolated from this tissue as described (Kaech and Banker 2006), with some modifications. Tissues were rinsed in ice-cold 2M glucose solution in PBS, incubated for 5 min at 37°C with a solution of 0.05% trypsin-EDTA and 250 U/ml DNase I (AM2222, Ambion) in glial medium [MEM (Gibco) supplemented with 0.6% glucose, penicillin/streptomycin, and 10% horse serum], and then mechanically dissociated with fire-polished glass Pasteur pipettes of decreasing diameters. After homogenization, cells were centrifuged for 5 min at 1,500 rpm, the supernatant was removed, and cells were resuspended in glial medium and plated in poly-D-lysine/laminin-coated T-25 bottles. Every 3-4 days, the cells were washed with PBS, and the culture medium was replaced. When reaching 80% confluency, cells were shaken at 60 rpm for 16 hours at 37°C with 5% CO_2 to remove microglia, and after passaging, the cells were seeded at 2.5 x 10^4 cells/cm^2 in poly-D-lysine/laminin-coated plates; the medium was replaced every 4 days. All experiments were performed using astrocytes at <20 passages.

Astrocytes were transfected with lentiviral vectors expressing shRNAs (see the “Lentivirus and retrovirus production” section below) using Lipofectamine 3000 reagent (Invitrogen), following the manufacturer's instructions. Twenty-four hours after transfection, cells were rinsed with PBS and cultured for 48 hours, in glial medium without horse serum. The media were harvested and centrifuged at 1,500 g for 5 min, and the supernatant was passed through

a 0.22 µm filter and precipitated with methanol/chloroform in a ratio of 1:1:0.25. Total cell lysates were prepared as described in the Western blot analysis section above.

Hippocampal NSCs/Astrocyte sandwich co-culture system

Co-cultures were obtained as previously described (Song et al. 2002; Kaech and Banker 2006), including the following modifications. Briefly, astrocytes were seeded in poly-D-lysine/laminin-coated culture plates at 2.5 x 10^4 cells per cm^2 for 4 days. In parallel, hippocampal NSCs were seeded onto poly-D-lysine/laminin-coated glass coverslips in 24-well culture plates at 2 x 10^4 cells per cm^2. After 24 hours, NSCs were mounted on 3D discs positioned on the astrocyte monolayer that had been previously cultured in NSC medium for 24 hours. The co-culture discs were 3D printed using dimensions to position a 12 mm coverslip with NSCs 2 mm above the astrocyte cultures (Supplemental Fig S3A).

For the proliferation experiments, co-cultures were maintained for 24 hours in the control condition or in the presence of the chimera proteins Fc-LGR4 (8077-GP, R&D Systems), Fc-LGR5 (8078-GP, R&D Systems), and Fc-Control (110-HG, R&D Systems) for 24 hours, and 10 µM BrdU was added for the last 4 hours of treatment. Proliferation was quantified as the percentage of BrdU-positive cells. For RSPO2 knockdown experiments, astrocytes were transfected with lentiviral vectors expressing shRNAs (see "Lentivirus and retrovirus production" section below) using Lipofectamine 3000 reagent (Invitrogen) following the manufacturer's instructions. Twenty-four hours post-transfection, the glial medium was replaced by NSCs medium, and after 24 hours, the co-cultures were mounted in the presence of growth factors. After another 24 hours, NSCs were fixed, and proliferation was quantified as the percentage of Ki67-positive cells.

For LGR5 knockdown experiments, NSCs were transduced for 48 hours with shRNA-expressing retroviruses (see "Lentivirus and retrovirus production" section below) and

subsequently co-cultured with or without astrocytes for 24 hours in the presence of growth factors. Proliferation was quantified as the percentage of Ki67-positive cells.

Lentivirus and retrovirus production

To knockdown RSPO2 and LGR5, inverted self-complementary hairpin DNA oligonucleotides encoding short-hairpin RNAs (shRNA) against mouse RSPO2 (shR1 and shR2) or LGR5 (shLGR5) were chemically synthesized. Oligos used to construct the shRNAs were: shR1: 5′-TG*CGAGCTAGTTATGTATCAAAT*TTCAAGAGAATTTGATACATAACTAGCTCGCTTTTTTC-3′; shR2: 5′-TG*AGCGAGCTAGTTATGTATCAA*TTCAAGAGATTGATACATAACTAGCTCGCTC-TTTTTTC-3′; shLGR5: 5′-GA*TCCGGCGAGTCTGCTGTCCATTAAC*TTCAAGAGAGTTAATGGACAGCAGACTCGCTTTTTTACGCGTG-3′. Target mRNA sequences are shown in italic. As a control, shRNA targeting luciferase mRNA (Varas-Godoy et al. 2018) was used. RSPO2 shRNAs were cloned into the pLentiLox 3.7 lentiviral vector (PLL3.7, AddGene), which co-expresses green fluorescent protein (GFP), and shLGR5 was cloned into the pSiren-RetroQ-ZsGreen vector (Clontech). For lentivirus preparation, $1x10^6$ HEK293T cells were seeded per 100 mm dish, once the cells reached 90% confluence (~3 days), cells were co-transfected with 14.4 µg pLentiLox vector containing the sequence of each shRNA, 9.2 µg pMDLg/pRRE vector encoding the gag and pol enzymes, 4.9 µg pVSV-G vector required for capsid formation, and 3.6 µg pRSV-Rev vector using 65 µL of PEImax (18 mM polyethylenimine, pH 7, Polysciences, Inc.). After 4 hours, the medium was replaced by fresh DMEM medium supplemented with 1% fetal bovine serum (FBS, Biowest) without antibiotics. The lentivirus-

containing supernatants were collected 72 hours post-transfection, and centrifuged twice at 2,000 g for 30 min at 4°C on AMICON filters (Ultra-15 Centrifugal Filter Unit). The concentrated viruses were aliquoted and stored at -80°C.

For retrovirus production $1x10^6$ HEK293T cells were seeded in 100 mm culture dishes, and once the cells reached 90% confluence (~3 days), they were co-transfected with 220 µL Optimem, 14.4 µg silencing vector, 9.2 µg pMDL g/p, 4.9 µg VSV-G, and 65 µL PEImax. The retroviral transfection mix was incubated for 10 min at room temperature, added dropwise onto the HEK293T cell medium, and left at 37ºC with 5% CO_2. After 4 hours, the medium was replaced by DMEM medium supplemented with 1% FBS. At 72 hours post-transfection, the supernatants were harvested and centrifuged at 2,000 g for 5 min at 4ºC. Next, the supernatants were filtered using 0.22 µm cellulose acetate filters and then underwent two rounds of ultracentrifugation: 19,000 rpm for 2 hours, and then at 21,900 rpm for 2 hours. The pellet was resuspended in PBS, aliquoted, and stored at -80ºC.

Statistical analysis

Statistical analyses were performed using Prism 10 software (GraphPad Software Inc.). Data normality was checked using the Shapiro-Wilk test. One sample t-test or Wilcoxon test was used for fold-change analyses. A two-way ANOVA followed by a Tukey's or Dunnett's multiple comparison test was used in experiments with two variables. $p<0.05$ was considered statistically significant. Data represent the mean ± SEM.

Competing interests

The authors declare that the research was conducted in the absence of any commercial or financial relationships that could be construed as a potential conflict of interest.

Acknowledgments

This work was supported by grants from ANID/FONDECYT (1190461 and 1230454, to LVN), Nucleo UNAB (DI-4-17/N, to LVN), ANID 21210618 to DVB, and ANID/FONDECYT postdoctoral grant (3230100, to SBA).

Author contributions: DV-B: conception and design, retrovirus production, acquisition, analysis, and interpretation of data. MDM: conception and design, and acquisition of data. MG: lentivirus production, data acquisition and analysis of co-culture experiments with RSPO2-deficient astrocytes. SBA: acquisition and analysis of data from RSPO2 knockdown. SHS: Lentivirus production and validation of RSPO2 knockdown. NM-V: design and production of the sandwich co-culture system. FJB: shRNAs design (RSPO2 and LGR5), lentivirus production, analysis, and interpretation of data. LV-N: conception and design, assembly and interpretation of data, manuscript writing, and financial support. All authors read and approved the final version of the paper.

REFERENCES

Abbott AC, Calderon Toledo C, Aranguiz FC, Inestrosa NC, Varela-Nallar L. 2013. Tetrahydrohyperforin increases adult hippocampal neurogenesis in wild-type and APPswe/PS1DeltaE9 mice. *J Alzheimers Dis* **34**: 873-885.

Amador-Arjona A, Cimadamore F, Huang CT, Wright R, Lewis S, Gage FH, Terskikh AV. 2015. SOX2 primes the epigenetic landscape in neural precursors enabling proper gene activation during hippocampal neurogenesis. *Proc Natl Acad Sci U S A* **112**: E1936-1945.

Anacker C, Hen R. 2017. Adult hippocampal neurogenesis and cognitive flexibility - linking memory and mood. *Nat Rev Neurosci* **18**: 335-346.

Arredondo SB, Guerrero FG, Herrera-Soto A, Jensen-Flores J, Bustamante DB, Onate-Ponce A, Henny P, Varas-Godoy M, Inestrosa NC, Varela-Nallar L. 2020a. Wnt5a promotes differentiation and development of adult-born neurons in the hippocampus by noncanonical Wnt signaling. *Stem Cells* **38**: 422-436.

Arredondo SB, Valenzuela-Bezanilla D, Mardones MD, Varela-Nallar L. 2020b. Role of Wnt Signaling in Adult Hippocampal Neurogenesis in Health and Disease. *Front Cell Dev Biol* **8**: 860.

Arredondo SB, Valenzuela-Bezanilla D, Santibanez SH, Varela-Nallar L. 2022. Wnt signaling in the adult hippocampal neurogenic niche. *Stem Cells*.

Austin SHL, Gabarro-Solanas R, Rigo P, Paun O, Harris L, Guillemot F, Urban N. 2021. Wnt/beta-catenin signalling is dispensable for adult neural stem cell homeostasis and activation. *Development* **148**.

Babu H, Claasen JH, Kannan S, Runker AE, Palmer T, Kempermann G. 2011. A protocol for isolation and enriched monolayer cultivation of neural precursor cells from mouse dentate gyrus. *Front Neurosci* **5**: 89.

Barker N, Huch M, Kujala P, van de Wetering M, Snippert HJ, van Es JH, Sato T, Stange DE, Begthel H, van den Born M et al. 2010. Lgr5(+ve) stem cells drive self-renewal in the stomach and build long-lived gastric units in vitro. *Cell Stem Cell* **6**: 25-36.

Barker N, van Es JH, Kuipers J, Kujala P, van den Born M, Cozijnsen M, Haegebarth A, Korving J, Begthel H, Peters PJ, Clevers H. 2007. Identification of stem cells in small intestine and colon by marker gene Lgr5. *Nature* **449**: 1003-1007.

Ben Abdallah NM, Slomianka L, Vyssotski AL, Lipp HP. 2010. Early age-related changes in adult hippocampal neurogenesis in C57 mice. *Neurobiol Aging* **31**: 151-161.

Blaas L, Pucci F, Messal HA, Andersson AB, Josue Ruiz E, Gerling M, Douagi I, Spencer-Dene B, Musch A, Mitter R et al. 2016. Lgr6 labels a rare population of mammary gland progenitor cells that are able to originate luminal mammary tumours. *Nat Cell Biol* **18**: 1346-1356.

Bonaguidi MA, Wheeler MA, Shapiro JS, Stadel RP, Sun GJ, Ming GL, Song H. 2011. In vivo clonal analysis reveals self-renewing and multipotent adult neural stem cell characteristics. *Cell* **145**: 1142-1155.

Butler MT, Wallingford JB. 2017. Planar cell polarity in development and disease. *Nat Rev Mol Cell Biol* **18**: 375-388.

Cao Y, Liu P, Bian H, Jin S, Liu J, Yu N, Cui H, Sun F, Qian X, Qiu W, Ma C. 2023. Reduced neurogenesis in human hippocampus with Alzheimer's disease. *Brain Pathol*: e13225.

Carmon KS, Gong X, Lin Q, Thomas A, Liu Q. 2011. R-spondins function as ligands of the orphan receptors LGR4 and LGR5 to regulate Wnt/beta-catenin signaling. *Proc Natl Acad Sci U S A* **108**: 11452-11457.

Casse F, Richetin K, Toni N. 2018. Astrocytes' Contribution to Adult Neurogenesis in Physiology and Alzheimer's Disease. *Front Cell Neurosci* **12**: 432.

Chang CF, Hsu LS, Weng CY, Chen CK, Wang SY, Chou YH, Liu YY, Yuan ZX, Huang WY, Lin H et al. 2016. N-Glycosylation of Human R-Spondin 1 Is Required for Efficient Secretion and Stability but Not for Its Heparin Binding Ability. *Int J Mol Sci* **17**.

Chaves-Perez A, Santos-de-Frutos K, de la Rosa S, Herranz-Montoya I, Perna C, Djouder N. 2022. Transit-amplifying cells control R-spondins in the mouse crypt to modulate intestinal stem cell proliferation. *J Exp Med* **219**.

Clevers H, Nusse R. 2012. Wnt/beta-catenin signaling and disease. *Cell* **149**: 1192-1205.

de Lau W, Barker N, Low TY, Koo BK, Li VS, Teunissen H, Kujala P, Haegebarth A, Peters PJ, van de Wetering M et al. 2011. Lgr5 homologues associate with Wnt receptors and mediate R-spondin signalling. *Nature* **476**: 293-297.

de Lau W, Peng WC, Gros P, Clevers H. 2014. The R-spondin/Lgr5/Rnf43 module: regulator of Wnt signal strength. *Genes Dev* **28**: 305-316.

de Lau WB, Snel B, Clevers HC. 2012. The R-spondin protein family. *Genome Biol* **13**: 242.

de Visser KE, Ciampricotti M, Michalak EM, Tan DW, Speksnijder EN, Hau CS, Clevers H, Barker N, Jonkers J. 2012. Developmental stage-specific contribution of LGR5(+) cells to basal and luminal epithelial lineages in the postnatal mammary gland. *J Pathol* **228**: 300-309.

Dunn SJ, Osborne JM, Appleton PL, Nathke I. 2016. Combined changes in Wnt signaling response and contact inhibition induce altered proliferation in radiation-treated intestinal crypts. *Mol Biol Cell* **27**: 1863-1874.

Encinas JM, Michurina TV, Peunova N, Park JH, Tordo J, Peterson DA, Fishell G, Koulakov A, Enikolopov G. 2011. Division-coupled astrocytic differentiation and age-related depletion of neural stem cells in the adult hippocampus. *Cell Stem Cell* **8**: 566-579.

Garbe DS, Ring RH. 2012. Investigating tonic Wnt signaling throughout the adult CNS and in the hippocampal neurogenic niche of BatGal and ins-TopGal mice. *Cell Mol Neurobiol* **32**: 1159-1174.

Glinka A, Dolde C, Kirsch N, Huang YL, Kazanskaya O, Ingelfinger D, Boutros M, Cruciat CM, Niehrs C. 2011. LGR4 and LGR5 are R-spondin receptors mediating Wnt/beta-catenin and Wnt/PCP signalling. *EMBO Rep* **12**: 1055-1061.

Gong X, Carmon KS, Lin Q, Thomas A, Yi J, Liu Q. 2012. LGR6 is a high affinity receptor of R-spondins and potentially functions as a tumor suppressor. *PLoS One* **7**: e37137.

Gordon MD, Nusse R. 2006. Wnt signaling: multiple pathways, multiple receptors, and multiple transcription factors. *J Biol Chem* **281**: 22429-22433.

Guerra MV, Caceres MI, Herrera-Soto A, Arredondo SB, Varas-Godoy M, van Zundert B, Varela-Nallar L. 2022. H3K9 Methyltransferases Suv39h1 and Suv39h2 Control the Differentiation of Neural Progenitor Cells in the Adult Hippocampus. *Front Cell Dev Biol* **9**: 778345.

Hagner A, Shin W, Sinha S, Alpaugh W, Workentine M, Abbasi S, Rahmani W, Agabalyan N, Sharma N, Sparks H et al. 2020. Transcriptional Profiling of the Adult Hair Follicle Mesenchyme Reveals R-spondin as a Novel Regulator of Dermal Progenitor Function. *iScience* **23**: 101019.

Hao HX, Jiang X, Cong F. 2016. Control of Wnt Receptor Turnover by R-spondin-ZNRF3/RNF43 Signaling Module and Its Dysregulation in Cancer. *Cancers (Basel)* **8**.

Hao HX, Xie Y, Zhang Y, Charlat O, Oster E, Avello M, Lei H, Mickanin C, Liu D, Ruffner H et al. 2012. ZNRF3 promotes Wnt receptor turnover in an R-spondin-sensitive manner. *Nature* **485**: 195-200.

Harnack C, Berger H, Antanaviciute A, Vidal R, Sauer S, Simmons A, Meyer TF, Sigal M. 2019. R-spondin 3 promotes stem cell recovery and epithelial regeneration in the colon. *Nat Commun* **10**: 4368.

Heppt J, Wittmann MT, Schaffner I, Billmann C, Zhang J, Vogt-Weisenhorn D, Prakash N, Wurst W, Taketo MM, Lie DC. 2020. beta-catenin signaling modulates the tempo of dendritic growth of adult-born hippocampal neurons. *EMBO J* **39**: e104472.

Jaks V, Barker N, Kasper M, van Es JH, Snippert HJ, Clevers H, Toftgard R. 2008. Lgr5 marks cycling, yet long-lived, hair follicle stem cells. *Nat Genet* **40**: 1291-1299.

Jho EH, Zhang T, Domon C, Joo CK, Freund JN, Costantini F. 2002. Wnt/beta-catenin/Tcf signaling induces the transcription of Axin2, a negative regulator of the signaling pathway. *Mol Cell Biol* **22**: 1172-1183.

Kaech S, Banker G. 2006. Culturing hippocampal neurons. *Nat Protoc* **1**: 2406-2415.

Kempermann G. 2022. What Is Adult Hippocampal Neurogenesis Good for? *Front Neurosci* **16**: 852680.

Kim KA, Kakitani M, Zhao J, Oshima T, Tang T, Binnerts M, Liu Y, Boyle B, Park E, Emtage P et al. 2005. Mitogenic influence of human R-spondin1 on the intestinal epithelium. *Science* **309**: 1256-1259.

Kim KA, Wagle M, Tran K, Zhan X, Dixon MA, Liu S, Gros D, Korver W, Yonkovich S, Tomasevic N et al. 2008. R-Spondin family members regulate the Wnt pathway by a common mechanism. *Mol Biol Cell* **19**: 2588-2596.

Kim KA, Zhao J, Andarmani S, Kakitani M, Oshima T, Binnerts ME, Abo A, Tomizuka K, Funk WD. 2006. R-Spondin proteins: a novel link to beta-catenin activation. *Cell Cycle* **5**: 23-26.

Knoth R, Singec I, Ditter M, Pantazis G, Capetian P, Meyer RP, Horvat V, Volk B, Kempermann G. 2010. Murine features of neurogenesis in the human hippocampus across the lifespan from 0 to 100 years. *PLoS One* **5**: e8809.

Kohn AD, Moon RT. 2005. Wnt and calcium signaling: beta-catenin-independent pathways. *Cell Calcium* **38**: 439-446.

Koo BK, Spit M, Jordens I, Low TY, Stange DE, van de Wetering M, van Es JH, Mohammed S, Heck AJ, Maurice MM, Clevers H. 2012. Tumour suppressor RNF43 is a stem-cell E3 ligase that induces endocytosis of Wnt receptors. *Nature* **488**: 665-669.

Kuwabara T, Hsieh J, Muotri A, Yeo G, Warashina M, Lie DC, Moore L, Nakashima K, Asashima M, Gage FH. 2009. Wnt-mediated activation of NeuroD1 and retro-elements during adult neurogenesis. *Nat Neurosci* **12**: 1097-1105.

Lee H, Seidl C, Sun R, Glinka A, Niehrs C. 2020. R-spondins are BMP receptor antagonists in Xenopus early embryonic development. *Nat Commun* **11**: 5570.

Lehoczky JA, Tabin CJ. 2015. Lgr6 marks nail stem cells and is required for digit tip regeneration. *Proc Natl Acad Sci U S A* **112**: 13249-13254.

Lein ES Hawrylycz MJ Ao N Ayres M Bensinger A Bernard A Boe AF Boguski MS Brockway KS Byrnes EJ et al. 2007. Genome-wide atlas of gene expression in the adult mouse brain. *Nature* **445**: 168-176.

Leung JY, Kolligs FT, Wu R, Zhai Y, Kuick R, Hanash S, Cho KR, Fearon ER. 2002. Activation of AXIN2 expression by beta-catenin-T cell factor. A feedback repressor pathway regulating Wnt signaling. *J Biol Chem* **277**: 21657-21665.

Lie DC, Colamarino SA, Song HJ, Desire L, Mira H, Consiglio A, Lein ES, Jessberger S, Lansford H, Dearie AR, Gage FH. 2005. Wnt signalling regulates adult hippocampal neurogenesis. *Nature* **437**: 1370-1375.

Liu W, Dong X, Mai M, Seelan RS, Taniguchi K, Krishnadath KK, Halling KC, Cunningham JM, Boardman LA, Qian C et al. 2000. Mutations in AXIN2 cause colorectal cancer with defective mismatch repair by activating beta-catenin/TCF signalling. *Nat Genet* **26**: 146-147.

Lustig B, Jerchow B, Sachs M, Weiler S, Pietsch T, Karsten U, van de Wetering M, Clevers H, Schlag PM, Birchmeier W, Behrens J. 2002. Negative feedback loop of Wnt signaling through upregulation of conductin/axin2 in colorectal and liver tumors. *Mol Cell Biol* **22**: 1184-1193.

Mao Y, Ge X, Frank CL, Madison JM, Koehler AN, Doud MK, Tassa C, Berry EM, Soda T, Singh KK et al. 2009. Disrupted in schizophrenia 1 regulates neuronal progenitor

proliferation via modulation of GSK3beta/beta-catenin signaling. *Cell* **136**: 1017-1031.

Miller TE, Wang J, Sukhdeo K, Horbinski C, Tesar PJ, Wechsler-Reya RJ, Rich JN. 2014. Lgr5 Marks Post-Mitotic, Lineage Restricted Cerebellar Granule Neurons during Postnatal Development. *PLoS One* **9**: e114433.

Moreno-Jimenez EP, Flor-Garcia M, Terreros-Roncal J, Rabano A, Cafini F, Pallas-Bazarra N, Avila J, Llorens-Martin M. 2019. Adult hippocampal neurogenesis is abundant in neurologically healthy subjects and drops sharply in patients with Alzheimer's disease. *Nat Med* **25**: 554-560.

Moss J, Gebara E, Bushong EA, Sanchez-Pascual I, O'Laoi R, El M'Ghari I, Kocher-Braissant J, Ellisman MH, Toni N. 2016. Fine processes of Nestin-GFP-positive radial glia-like stem cells in the adult dentate gyrus ensheathe local synapses and vasculature. *Proc Natl Acad Sci U S A* **113**: E2536-2545.

Mustata RC, Van Loy T, Lefort A, Libert F, Strollo S, Vassart G, Garcia MI. 2011. Lgr4 is required for Paneth cell differentiation and maintenance of intestinal stem cells ex vivo. *EMBO Rep* **12**: 558-564.

Nagano K. 2019. R-spondin signaling as a pivotal regulator of tissue development and homeostasis. *Jpn Dent Sci Rev* **55**: 80-87.

Nam JS, Turcotte TJ, Yoon JK. 2007. Dynamic expression of R-spondin family genes in mouse development. *Gene Expr Patterns* **7**: 306-312.

Nusse R, Clevers H. 2017. Wnt/beta-Catenin Signaling, Disease, and Emerging Therapeutic Modalities. *Cell* **169**: 985-999.

Ohkawara B, Glinka A, Niehrs C. 2011. Rspo3 binds syndecan 4 and induces Wnt/PCP signaling via clathrin-mediated endocytosis to promote morphogenesis. *Dev Cell* **20**: 303-314.

Okamoto M, Inoue K, Iwamura H, Terashima K, Soya H, Asashima M, Kuwabara T. 2011. Reduction in paracrine Wnt3 factors during aging causes impaired adult neurogenesis. *FASEB J* **25**: 3570-3582.

Qu Q, Sun G, Murai K, Ye P, Li W, Asuelime G, Cheung YT, Shi Y. 2013. Wnt7a regulates multiple steps of neurogenesis. *Mol Cell Biol* **33**: 2551-2559.

Rao X, Huang X, Zhou Z, Lin X. 2013. An improvement of the 2^(-delta delta CT) method for quantitative real-time polymerase chain reaction data analysis. *Biostat Bioinforma Biomath* **3**: 71-85.

Raslan AA, Oh YJ, Jin YR, Yoon JK. 2022. R-Spondin2, a Positive Canonical WNT Signaling Regulator, Controls the Expansion and Differentiation of Distal Lung Epithelial Stem/Progenitor Cells in Mice. *Int J Mol Sci* **23**.

Rieskamp JD, Sarchet P, Smith BM, Kirby ED. 2022. Estimation of the density of neural, glial, and endothelial lineage cells in the adult mouse dentate gyrus. *Neural Regen Res* **17**: 1286-1292.

Rosenbloom AB, Tarczynski M, Lam N, Kane RS, Bugaj LJ, Schaffer DV. 2020. beta-Catenin signaling dynamics regulate cell fate in differentiating neural stem cells. *Proc Natl Acad Sci U S A* **117**: 28828-28837.

Schafer ST, Han J, Pena M, von Bohlen Und Halbach O, Peters J, Gage FH. 2015. The Wnt adaptor protein ATP6AP2 regulates multiple stages of adult hippocampal neurogenesis. *J Neurosci* **35**: 4983-4998.

Schneider J, Karpf J, Beckervordersandforth R. 2019. Role of Astrocytes in the Neurogenic Niches. *Methods Mol Biol* **1938**: 19-33.

Scholz B, Korn C, Wojtarowicz J, Mogler C, Augustin I, Boutros M, Niehrs C, Augustin HG. 2016. Endothelial RSPO3 Controls Vascular Stability and Pruning through Non-canonical WNT/Ca(2+)/NFAT Signaling. *Dev Cell* **36**: 79-93.

Schuijers J, Clevers H. 2012. Adult mammalian stem cells: the role of Wnt, Lgr5 and R-spondins. *EMBO J* **31**: 2685-2696.

Shin J, Berg DA, Zhu Y, Shin JY, Song J, Bonaguidi MA, Enikolopov G, Nauen DW, Christian KM, Ming GL, Song H. 2015. Single-Cell RNA-Seq with Waterfall Reveals Molecular Cascades underlying Adult Neurogenesis. *Cell Stem Cell* **17**: 360-372.

Shtutman M, Zhurinsky J, Simcha I, Albanese C, D'Amico M, Pestell R, Ben-Ze'ev A. 1999. The cyclin D1 gene is a target of the beta-catenin/LEF-1 pathway. *Proc Natl Acad Sci U S A* **96**: 5522-5527.

Sigal M, Logan CY, Kapalczynska M, Mollenkopf HJ, Berger H, Wiedenmann B, Nusse R, Amieva MR, Meyer TF. 2017. Stromal R-spondin orchestrates gastric epithelial stem cells and gland homeostasis. *Nature* **548**: 451-455.

Sigal M, Reines MDM, Mullerke S, Fischer C, Kapalczynska M, Berger H, Bakker ERM, Mollenkopf HJ, Rothenberg ME, Wiedenmann B et al. 2019. R-spondin-3 induces secretory, antimicrobial Lgr5(+) cells in the stomach. *Nat Cell Biol* **21**: 812-823.

Song H, Stevens CF, Gage FH. 2002. Astroglia induce neurogenesis from adult neural stem cells. *Nature* **417**: 39-44.

Sultan S, Li L, Moss J, Petrelli F, Casse F, Gebara E, Lopatar J, Pfrieger FW, Bezzi P, Bischofberger J, Toni N. 2015. Synaptic Integration of Adult-Born Hippocampal Neurons Is Locally Controlled by Astrocytes. *Neuron* **88**: 957-972.

Ter Steege EJ, Bakker ERM. 2021. The role of R-spondin proteins in cancer biology. *Oncogene* **40**: 6469-6478.

Terreros-Roncal J, Moreno-Jimenez EP, Flor-Garcia M, Rodriguez-Moreno CB, Trinchero MF, Cafini F, Rabano A, Llorens-Martin M. 2021. Impact of neurodegenerative diseases on human adult hippocampal neurogenesis. *Science* **374**: 1106-1113.

Tobin MK, Musaraca K, Disouky A, Shetti A, Bheri A, Honer WG, Kim N, Dawe RJ, Bennett DA, Arfanakis K, Lazarov O. 2019. Human Hippocampal Neurogenesis Persists in Aged Adults and Alzheimer's Disease Patients. *Cell Stem Cell* **24**: 974-982 e973.

Toda T, Gage FH. 2018. Review: adult neurogenesis contributes to hippocampal plasticity. *Cell Tissue Res* **373**: 693-709.

Tsakiridis A, Huang Y, Blin G, Skylaki S, Wymeersch F, Osorno R, Economou C, Karagianni E, Zhao S, Lowell S, Wilson V. 2014. Distinct Wnt-driven primitive streak-like populations reflect in vivo lineage precursors. *Development* **141**: 1209-1221.

Urban N, Cheung TH. 2021. Stem cell quiescence: the challenging path to activation. *Development* **148**.

Van Schoore G, Mendive F, Pochet R, Vassart G. 2005. Expression pattern of the orphan receptor LGR4/GPR48 gene in the mouse. *Histochem Cell Biol* **124**: 35-50.

Varas-Godoy M, Lladser A, Farfan N, Villota C, Villegas J, Tapia JC, Burzio LO, Burzio VA, Valenzuela PDT. 2018. In vivo knockdown of antisense non-coding mitochondrial RNAs by a lentiviral-encoded shRNA inhibits melanoma tumor growth and lung colonization. *Pigment Cell Melanoma Res* **31**: 64-72.

Varela-Nallar L, Grabowski CP, Alfaro IE, Alvarez AR, Inestrosa NC. 2009. Role of the Wnt receptor Frizzled-1 in presynaptic differentiation and function. *Neural Dev* **4**: 41.

Varela-Nallar L, Rojas-Abalos M, Abbott AC, Moya EA, Iturriaga R, Inestrosa NC. 2014. Chronic hypoxia induces the activation of the Wnt/beta-catenin signaling pathway and stimulates hippocampal neurogenesis in wild-type and APPswe-PS1DeltaE9 transgenic mice in vivo. *Front Cell Neurosci* **8**: 17.

Walker TL, Kempermann G. 2014. One mouse, two cultures: isolation and culture of adult neural stem cells from the two neurogenic zones of individual mice. *J Vis Exp*: e51225.

Wang Y, Dong J, Li D, Lai L, Siwko S, Li Y, Liu M. 2013. Lgr4 regulates mammary gland development and stem cell activity through the pluripotency transcription factor Sox2. *Stem Cells* **31**: 1921-1931.

Wexler EM, Paucer A, Kornblum HI, Palmer TD, Geschwind DH. 2009. Endogenous Wnt signaling maintains neural progenitor cell potency. *Stem Cells* **27**: 1130-1141.

Yan KS, Janda CY, Chang J, Zheng GXY, Larkin KA, Luca VC, Chia LA, Mah AT, Han A, Terry JM et al. 2017. Non-equivalence of Wnt and R-spondin ligands during Lgr5(+) intestinal stem-cell self-renewal. *Nature* **545**: 238-242.

Yu Y, Moberly AH, Bhattarai JP, Duan C, Zheng Q, Li F, Huang H, Olson W, Luo W, Wen T et al. 2017. The Stem Cell Marker Lgr5 Defines a Subset of Postmitotic Neurons in the Olfactory Bulb. *J Neurosci* **37**: 9403-9414.

Zebisch M, Jones EY. 2015. ZNRF3/RNF43--A direct linkage of extracellular recognition and E3 ligase activity to modulate cell surface signalling. *Prog Biophys Mol Biol* **118**: 112-118.

Zebisch M, Xu Y, Krastev C, MacDonald BT, Chen M, Gilbert RJ, He X, Jones EY. 2013. Structural and molecular basis of ZNRF3/RNF43 transmembrane ubiquitin ligase inhibition by the Wnt agonist R-spondin. *Nat Commun* **4**: 2787.

Zhang Z, Broderick C, Nishimoto M, Yamaguchi T, Lee SJ, Zhang H, Chen H, Patel M, Ye J, Ponce A et al. 2020. Tissue-targeted R-spondin mimetics for liver regeneration. *Sci Rep* **10**: 13951.

Zhao C, Teng EM, Summers RG, Jr., Ming GL, Gage FH. 2006. Distinct morphological stages of dentate granule neuron maturation in the adult mouse hippocampus. *J Neurosci* **26**: 3-11.

Zhao J, Kim KA, De Vera J, Palencia S, Wagle M, Abo A. 2009. R-Spondin1 protects mice from chemotherapy or radiation-induced oral mucositis through the canonical Wnt/beta-catenin pathway. *Proc Natl Acad Sci U S A* **106**: 2331-2336.

Zhou Y, Su Y, Li S, Kennedy BC, Zhang DY, Bond AM, Sun Y, Jacob F, Lu L, Hu P et al. 2022. Molecular landscapes of human hippocampal immature neurons across lifespan. *Nature* **607**: 527-533.

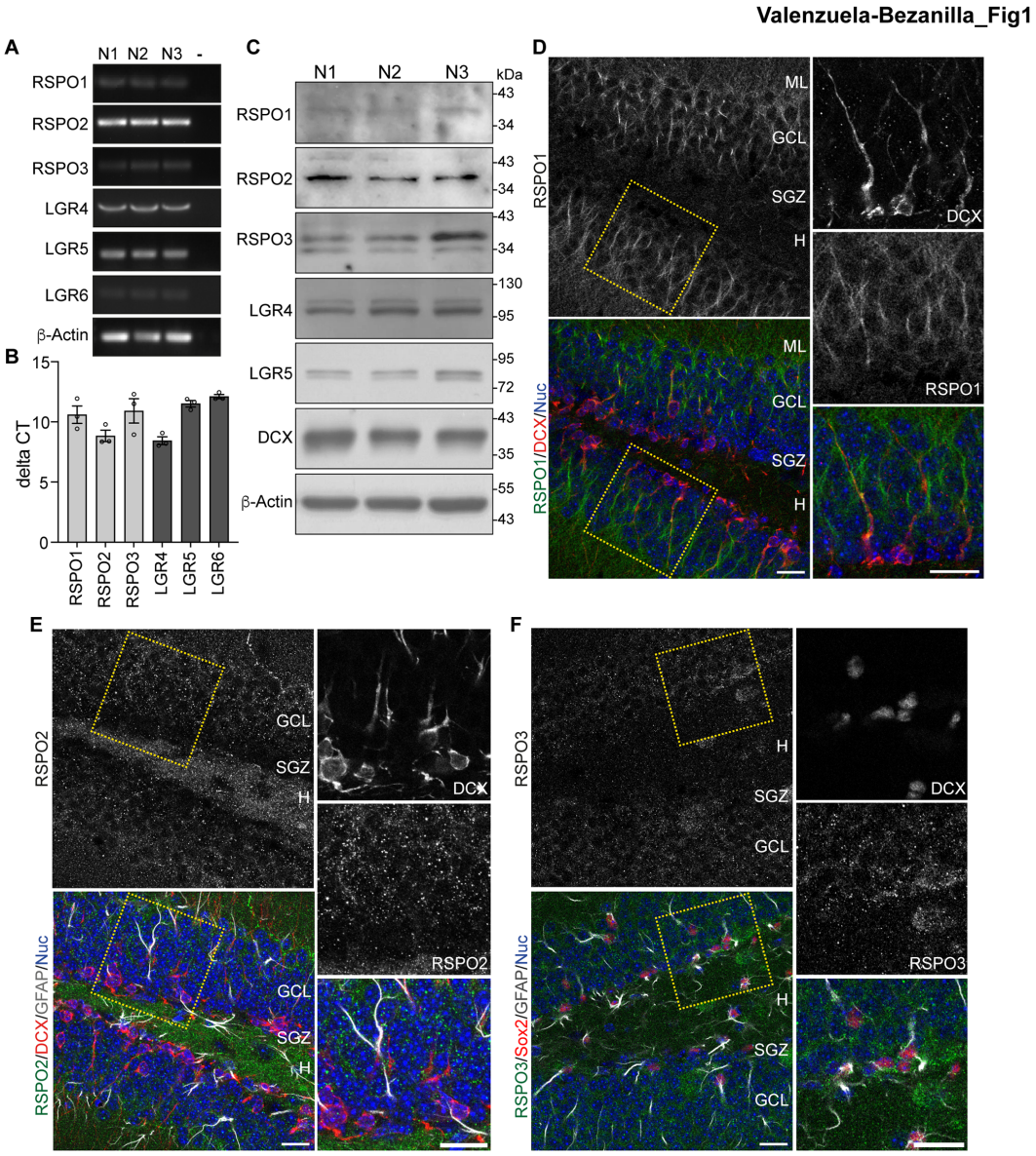

Figure 1. RSPO proteins and LGR receptors are expressed in the dentate gyrus of the adult mouse brain. (A, B) RT-qPCR from total RNA isolated from the dentate gyrus of 2-month-old mice. (A) End-point RT-qPCR reaction products. (B) delta CT values normalized to β-actin used as a reference gene. Of note, the lower the delta Ct value, the higher the expression of the gene. Bars show mean ± SEM. Dots show individual data (each one corresponds to 2 mice; total 6 mice). (C) Immunoblot from total protein extracts of the dentate gyrus of 2-month-old mice. Each N represents a pool of extracts from two animals. Numbers on the right indicate molecular weight standards (kDa). (D-F) Representative immunofluorescence staining of RSPO1 (C), RSPO2 (D), and RSPO3 (E) in the dentate gyrus of a 2-month-old mouse. Higher magnifications of the dotted squares are shown at the right. Scale bars: 20 µm. Immunodetection of DCX (red) was used as a marker of immature neurons in C and D; and GFAP (gray) and Sox2 (red) were used as markers of NSCs and astrocytes in E. NucBlue (Nuc, blue) was used for nuclear staining. GCL: granule cell layer; ML: molecular layer; SGZ: subgranular zone; H: Hilus.

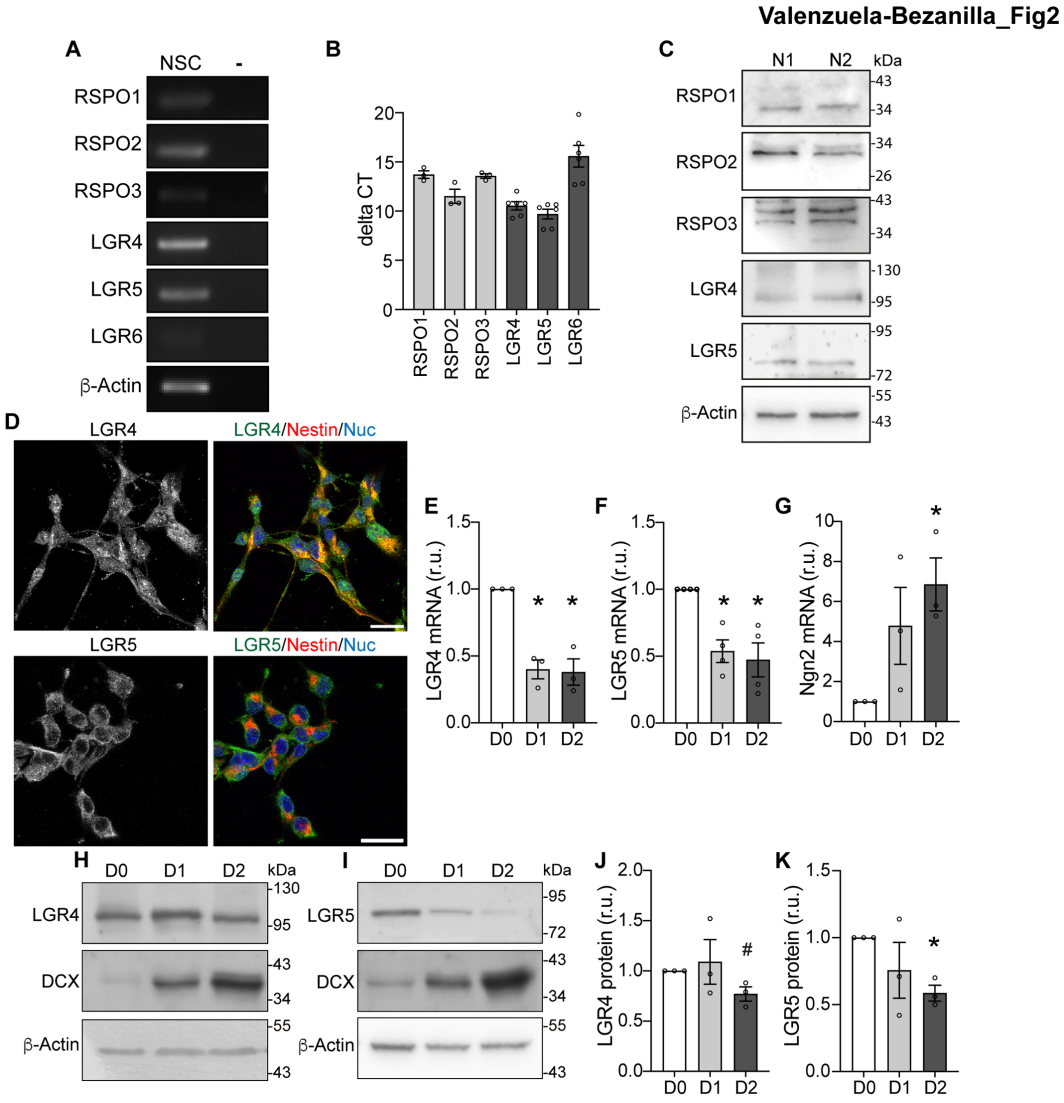

Figure 2. Expression of RSPO proteins and LGR receptors in cultured adult hippocampal NSCs. (A, B) RT-qPCR from total RNA isolated from cultured NSCs. End-point RT-qPCR reaction products (A) and delta CT values normalized to β-actin (B) are shown. Of note, the lower the delta Ct value, the higher the expression of the gene. Bars show mean ± SEM. (C) Immunoblot from total protein extracts of NSCs. The numbers on the right indicate the molecular weight standards (kDa). (D) Representative immunofluorescence staining of LGR4 or LGR5 (green), Nestin (red), and the nuclear staining NucBlue (Nuc, blue). Scale bar: 20 µm (E-G) RT-qPCR from total RNA isolated from NSCs under proliferative conditions (D0) and 24 (D1) or 48 (D2) hours after inducing differentiation by growth factor withdrawal. The mRNA levels of LGR4, LGR5, and Ngn2 (used as differentiation control) were normalized to β-actin mRNA and expressed relative to D0. (H-I) Immunoblot analysis of LGR4-5 in total protein extracts from NSCs at D0, D1, and D2. DCX was used as a neuronal differentiation control. (J-K) Densitometric analysis of LGR4-5 and DCX was normalized to β-actin and expressed relative to D0. Bars show mean ± SEM, and dots represent independent experiments. A one-sample t-test and Wilcoxon test were used. *$p < 0.05$, #$p < 0.08$.

Valenzuela-Bezanilla_Fig3

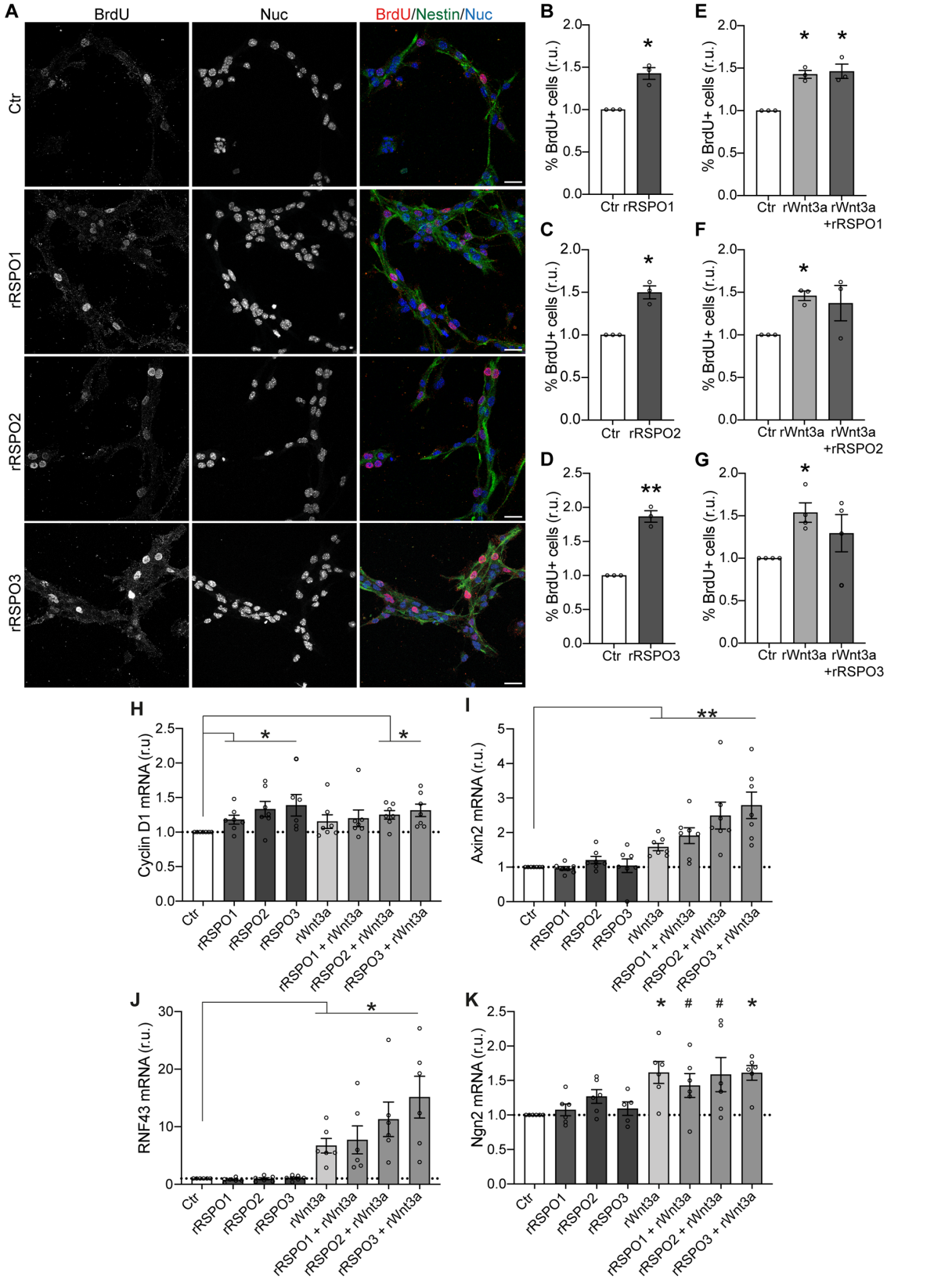

Figure 3. Treatment with RSPO proteins induces the proliferation of hippocampal NSCs and the expression of Wnt target genes. (A) Representative immunofluorescence staining of BrdU (red), Nestin (green) and Nuc (blue) in NSCs incubated for 24 hours in the presence or absence of 100 ng/ml recombinant RSPO1 (rRSPO1), rRSPO2, or rRSPO3 and were incubated with 10 μM BrdU for the last 2 hours of treatment. Scale bar: 20 μm. (B-G) Quantification of the percentage of BrdU positive NSCs treated with 100 ng/ml rRSPO1-3 (B-D) and 150 ng/ml of rWnt3a ± 100 ng/ml of rRSPO1-3 (E-G). Data are presented as fold-change relative to the control condition. Representative immunostaining of NSCs treated with rWnt3a ± rRSPO1-3 are shown in Supplemental Fig. 2. (H-K) RT-qPCR from total RNA isolated from NSCs treated for 24 hours with 100 ng/ml rRSPO1-3 or 150 ng/ml rWnt3a ± 100 ng/ml rRSPO1-3. Bars show mean ± SEM, and dots represent independent experiments. A one-sample t test and Wilcoxon test were used to compare all conditions versus the control condition. Kruskal-Wallis test was used for multiple comparisons. *$p<0.05$, **$p<0.01$, ***$p<0.001$, #$p<0.06$.

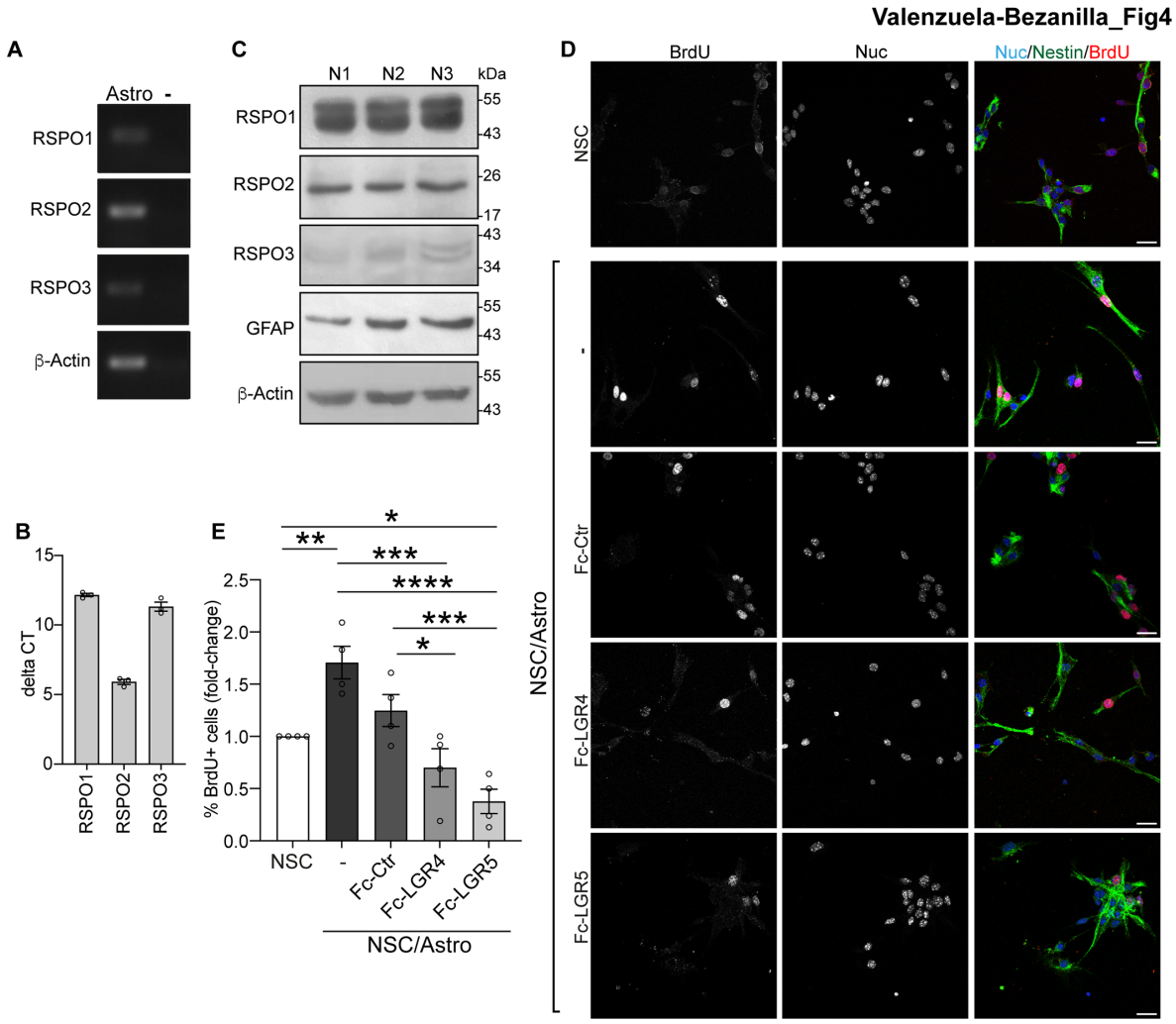

Figure 4. Cultured dentate gyrus astrocytes express RSPO proteins and induce proliferation of adult hippocampal NSCs in an RSPO-dependent manner. (A, B) RT-qPCR from total RNA isolated from primary cultured astrocytes isolated from the dentate gyrus of adult mice. End-point RT-qPCR reaction products (A) and delta CT values normalized to β-actin (B) are shown. Bars show mean ± SEM. (C) Immunoblot of total protein extracts from dentate gyrus astrocytes. Extracts from three different animals (N1–N3) are shown. The numbers on the right indicate the molecular weight standards (kDa). (D) Representative immunodetection of BrdU (red), Nestin (green), and Nuc (blue) in NSCs that were co-cultured (NSC/Astro) or not (NSC) with astrocytes for 24 hours in the presence or absence of 0.25 µg/ml Fc-LGR4, Fc-LGR5, or a control Fc (Fc-Ctrl) chimera, and BrdU was incorporated for the last 4 hours before fixation. Scale bar: 20 µm. (E) Percentage of cells positive for BrdU. Data are presented as fold-change relative to NSCs not co-cultured with astrocytes. Bars show mean ± SEM, and dots represent independent experiments. Two-way ANOVA followed by a Tukey's multiple comparison test was used. *p<0.05, **p<0.01, ***p<0.001, and ****p<0.0001.

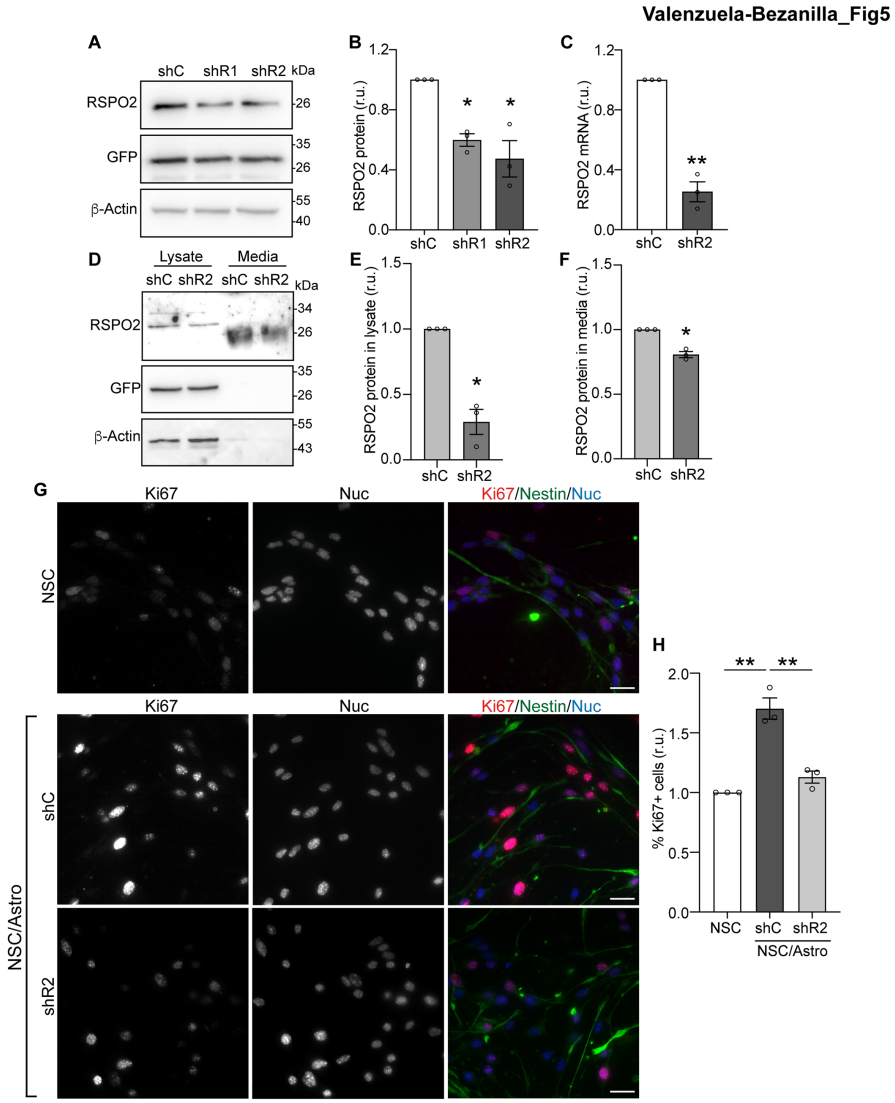

Figure 5. RSPO2 knockodown reduces astrocyte capacity to induce the proliferation of hippocampal NSCs. (A) Immunoblot of RSPO2 in the total protein extract of N2a cells transduced with lentivirus expressing shRNAs targeting RSPO2 (shR1, shR2) or a control shRNA (shC) and the reporter protein GFP. (B) Densitometric analysis of the immunoblots. RSPO2 protein levels were normalized to β-actin and expressed relative to shC. (C) RT-qPCR from total RNA isolated from N2a cells transduced for 72 hours with shR2 or shC. RSPO2 mRNA was normalized to β-actin mRNA and expressed relative to shC. (D) Immunoblot in total protein extracts (lysates) or the media of dentate gyrus astrocytes 72 hours after transfection with shR2 or shC vectors. (E-F) Densitometric analysis of the immunoblots. RSPO2 protein levels in the lysate were normalized to β-actin. RSPO2 levels in the lysates and media are expressed relative to the shC condition. (G) Representative immunodetection of Ki67 and Nestin in NSCs with or without co-culture for 24 hours with astrocytes transfected with shC or shR2. NucBlue (Nuc) was used as a nuclear marker. (H) Percentage of Ki67+ cells. Bars represent the mean ± SEM. Dots represent independent experiments. One-sample t-test and Wilcoxon test (B, C, E, F), or Two-way ANOVA followed by Tukey's multiple comparison test (H) were used. *p<0.05, **p<0.01.

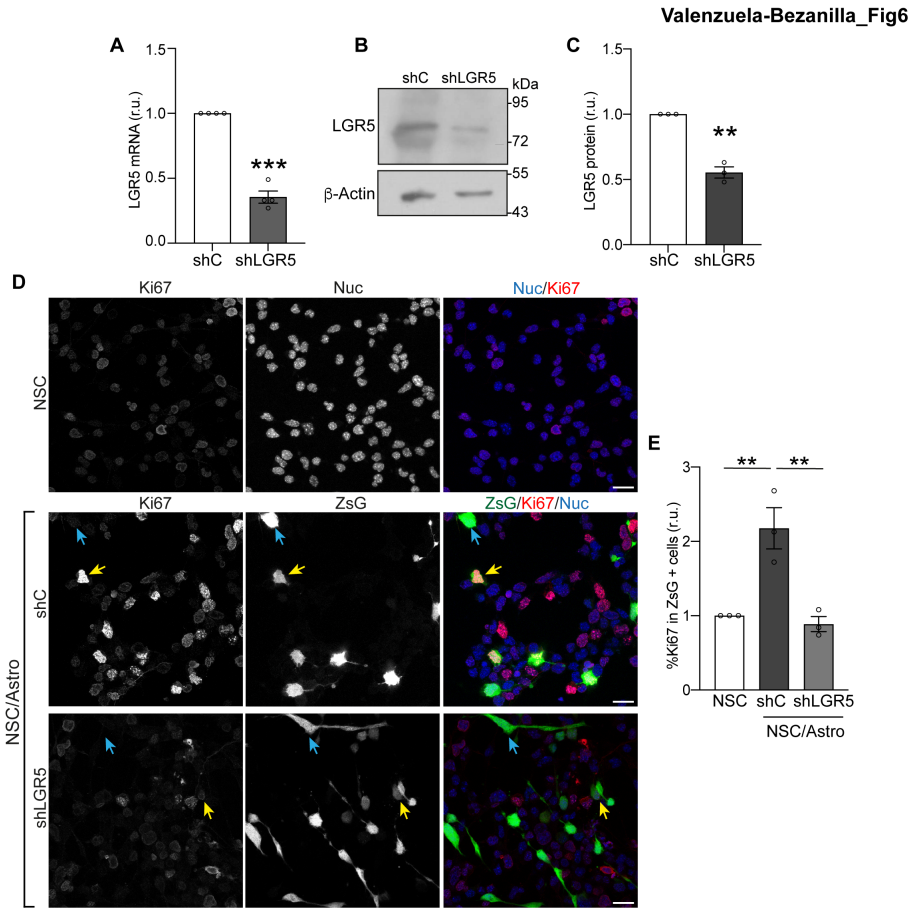

Figure 6. LGR5-deficient hippocampal NSCs have a reduced proliferative response to co-culture with dentate gyrus astrocytes. (A) RT-qPCR from total RNA isolated from NSCs transduced with a retrovirus expressing shRNA targeting LGR5 (shLGR5) or a control shRNA (shC) and the reporter protein ZsG. LGR5 mRNA was normalized to β-actin mRNA and expressed relative to shC. (B) Immunoblot of total protein extracts of NSCs 72 hours after transduction with the retroviruses. (C) Densitometric analysis of the immunoblots. LGR5 protein levels were normalized to β-actin protein levels and expressed relative to the shC condition. (D) Representative immunofluorescence staining of Ki67 in shRNA-transduced cells (ZsG+) in hippocampal NSCs with or without co-culture with astrocytes for 24 hours. Yellow arrows indicate ZsG+Ki67+ cells and blue arrows indicate ZsG+Ki67- cells. (E) Percentage of ZsG+ cells positive for Ki67. Bars represent the mean ± SEM. Dots represent independent experiments. One-sample t test and Wilcoxon test (A, C) or Two-way ANOVA and Tukey`s post-hoc test (E) were used. **p<0.01, ***p<0.001.